

Quantum technologies in Ireland: entangled photon emission from scalable arrays of site-controlled quantum dots

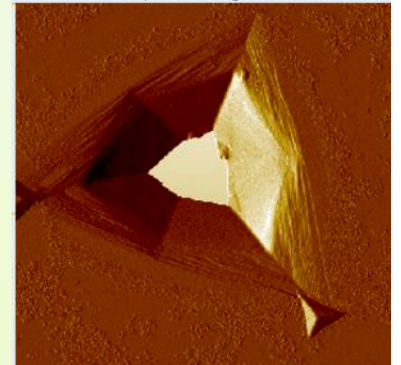
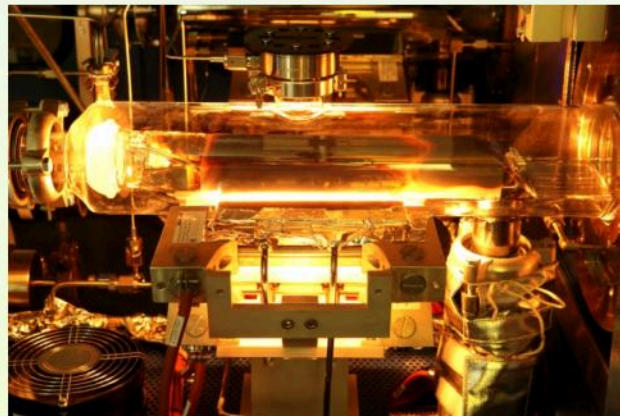
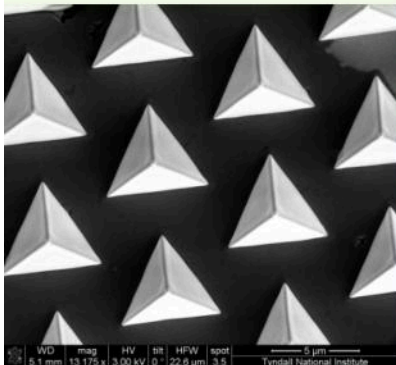
E. Pelucchi



**Collaborators: T. H. Chung, G. Juska, V. Dimastrodonato,
S. T. Moroni, A. Pescaglini, and A. Gocalinska**



***Epitaxy and Physics of Nanostructures,
Tyndall National Institute, University College Cork,
"Lee Maltings", Dyke Parade , Cork, Ireland***

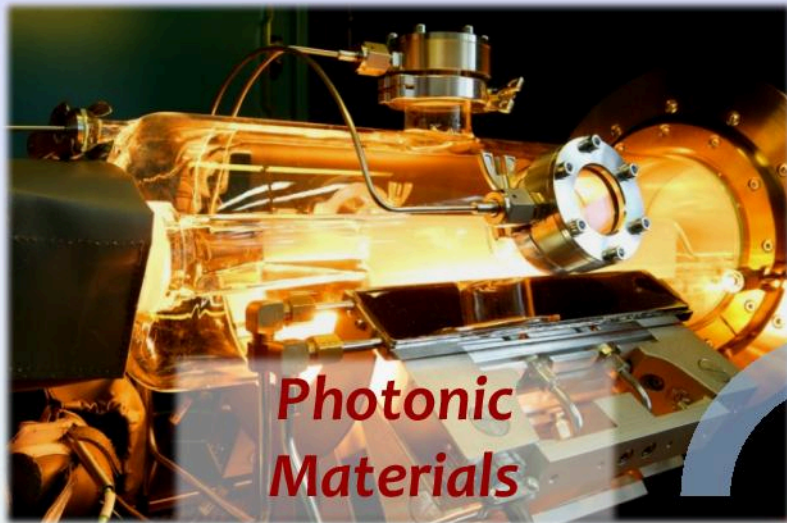


Tyndall (at University College Cork)

Excellence in ICT research



Tyndall Photonics Research Capabilities



For the moment Tyndall is the only place in Ireland with experimental quantum information

W

SINGLE PHOTON INTERFERENCE IN 10km LONG OPTICAL FIBRE INTERFEROMETER

P. D. Townsend, J. G. Rarity and P. R. Tapster

Indexing terms: Interferometers, Optical communication, Cryptography

Single-photon interference fringes with greater than 90% visibility were measured using a 10 km long optical fibre interferometer. The experiment employed a pulsed semiconductor laser source operating at a wavelength of $1.3 \mu\text{m}$ and a novel single-photon counting scheme using high-speed germanium avalanche photodiodes. Interferometers of this type could form the basis of future quantum cryptography systems.



P. Townsend has pioneered quantum cryptography

The security of any key-based cryptography system depends ultimately on the secrecy of the key. Quantum cryptography is a radical new technique for the distribution of cryptographic keys which exploits the uncertainty principle of quantum mechanics to guarantee the secrecy of the key [1-5]. The implementation of this technique in the optical domain involves the transmission of a random bit sequence from a source A to a receiver B using a single photon to carry each bit of data. This binary data can be encoded using, for example, either the polarisation states [1-4] or phase states of the photons [6, 7]. Random switching between orthogonal phase or polarisation coding bases provides protection against eavesdroppers. In performing measurements on the channel, an eavesdropper causes unavoidable changes in the photon states which show up as errors when A and B perform a comparison of a fraction of the sent and received bits. If the legitimate users of the channel fail to detect an eavesdropper they can use the remaining data to generate a cryptographic key. Unlike in conventional key distribution techniques, the secrecy of the key is now guaranteed by the fundamental laws of physics.

In a recent pioneering experiment, Bennett *et al.* [1] have demonstrated the operation of a quantum cryptographic channel, which was used to transmit a secret key over a free-space link about 30 cm in length at a data rate of approximately 10 bit/s. In this Letter, we characterise the performance of an optical-fibre-based single-photon communication channel which possesses some of the important features that the transmission medium for a future quantum cryptographic system would require. As illustrated in Fig. 1, the channel takes the form of an extended time-division Mach-Zehnder interferometer [6]. In this format, the Mach-Zehnder can be very long and yet remain stable against

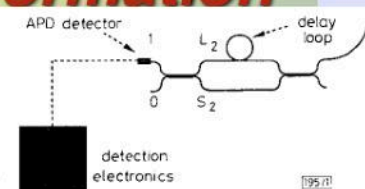
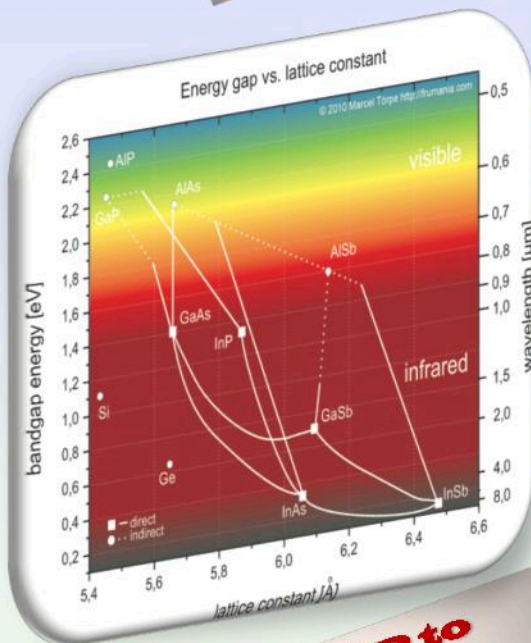


Fig. 1 Schematic diagram of single-photon time-division Mach-Zehnder interferometer

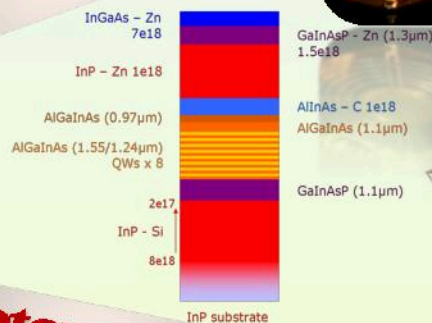
The source used in the experiment was a gain-switched semiconductor laser operating at a wavelength of $1.3 \mu\text{m}$, which produced pulses of 30 ps duration at a repetition rate of 105 MHz. The output from this laser was strongly attenuated so that at the input to the transmission fibre the average number of photons per pulse μ was of the order of 0.1. This choice of a small μ value was required to obtain a reasonable approximation to a single photon source. In this case a laser exhibiting Poissonian photon number fluctuations produces only a small fraction of pulses $\sim \mu^2/2$ containing on average two or more photons. However, this situation is obtained at the expense of a large fraction of pulses $\sim (1 - \mu)$ containing on average zero photons [1]. After attenuation, the incoming pulses were split by the first fibre-coupler (nominally 50/50) between a short fibre path S_1 , and a longer fibre path L_1 , in order to form a temporally separated pulse pair. Path L_1 contained a phase shifter consisting of a short free space link the length of which could be varied by means of a piezoelectric transducer (PZT). The path lengths L_1 and S_1 were chosen such that a relative time delay of 1.1 ns was obtained between the pair of pulses coupled into the transmission fibre via the second coupler. After propagation through 10 km of standard communications fibre, the pulses were again split between short and long paths of length $S_2 (=S_1)$ and $L_2 (=L_1)$, respectively, and then combined at the final coupler. The output from the final coupler thus consisted of three temporal pulses each separated by 1.1 ns. The central pulse was made up of two temporally coincident components that arrived via the S_1L_2 and the L_1S_2 paths, respectively, and hence exhibited interference behaviour as the relative optical phase was varied by means of the PZT.

Single photon counting was carried out using a high-speed germanium avalanche photodiode cooled to 77 K and operating in the Geiger mode with passive quenching via a 33 k Ω resistor [8]. After amplification and leading edge-discrimination, the signals from the detector were used as start pulses for a time-interval analyser (HP 53310A). For each

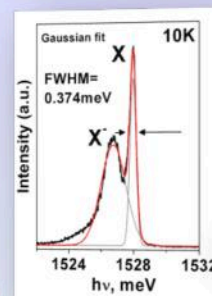
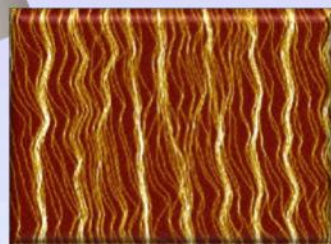
Growth Modelling



From AlP to InSb

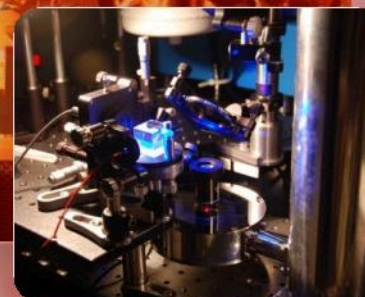
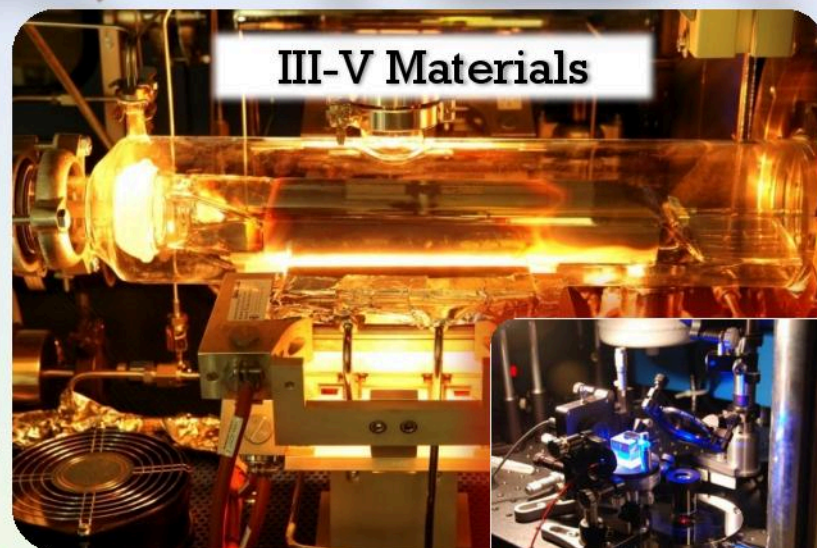


Photonic integration



High purity materials

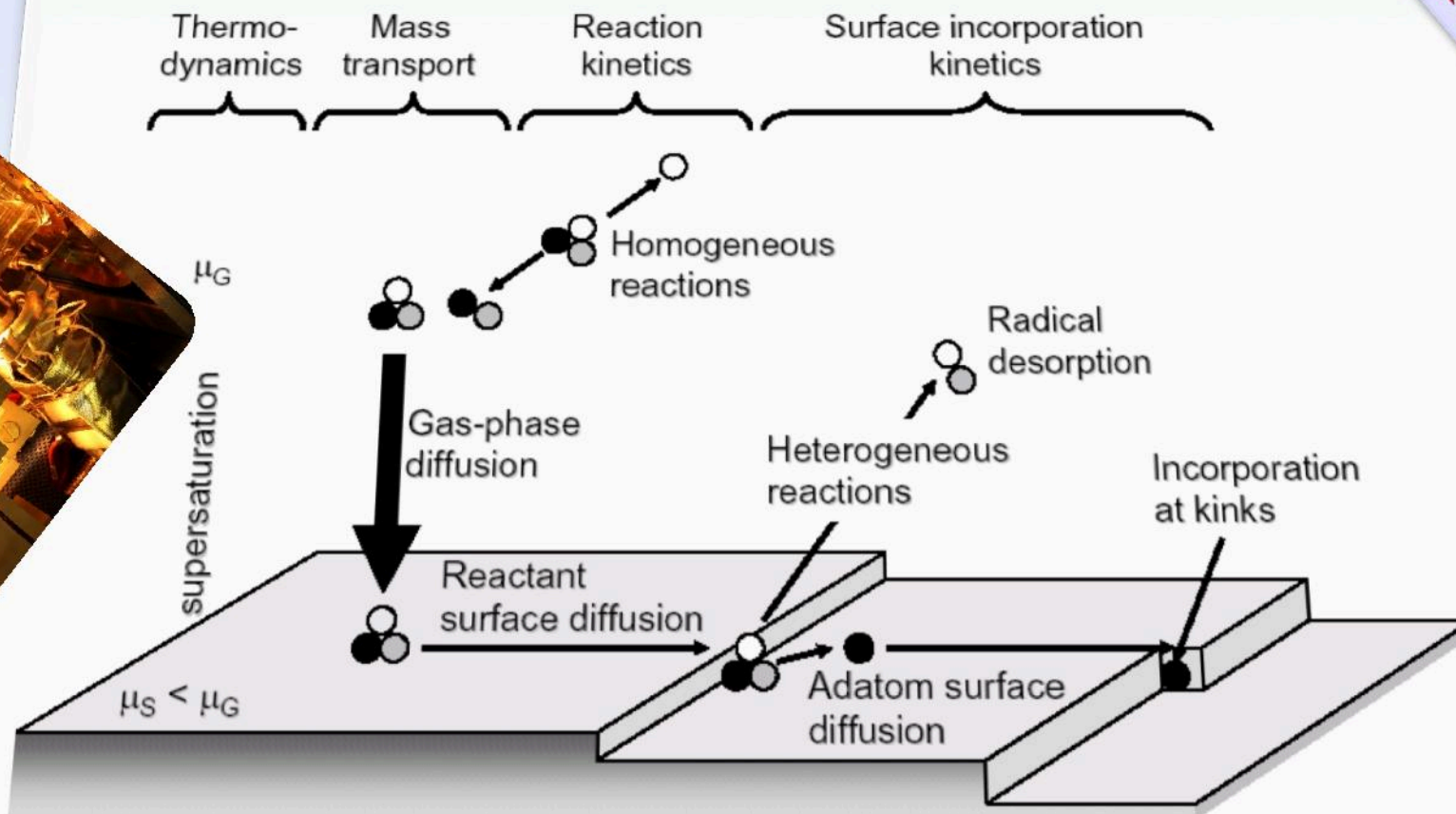
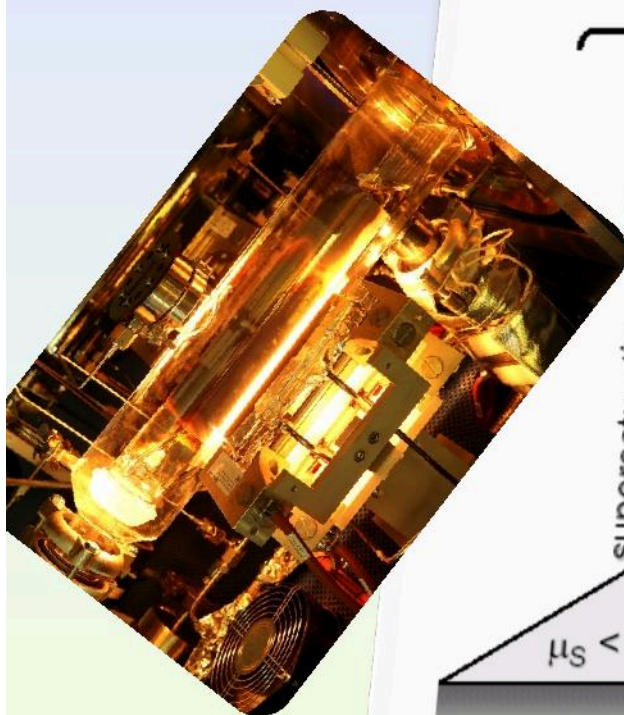
Metamorphic buffers and MOSFETs



Single QDs+ non-classical light

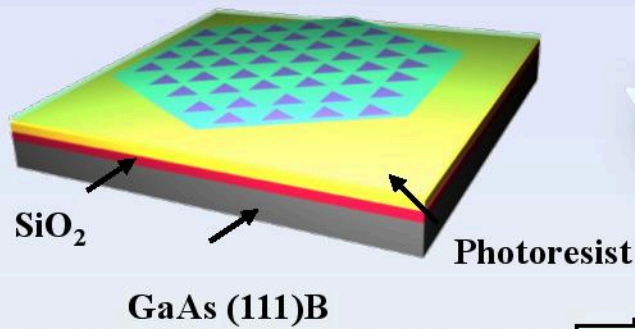
Double reactor set-up: single wafer for high purity and 3x2inch for device growths

A quick reminder



Our single quantum dots (which sometimes are actually decent “artificial atoms”.....)..
and the “second quantum revolution”...😊

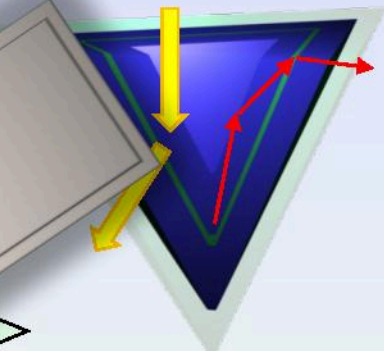
(111)B substrate patterning;
(photo)lithography+wet etching



MOVPE growth:
QW like

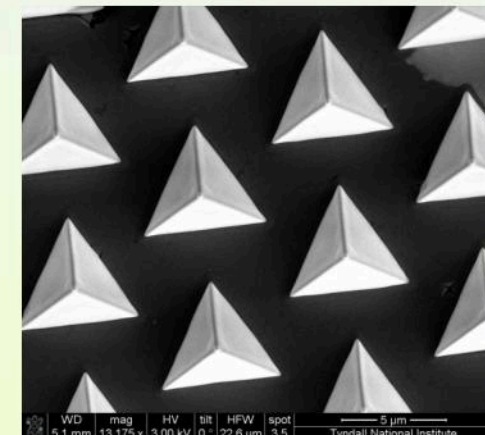
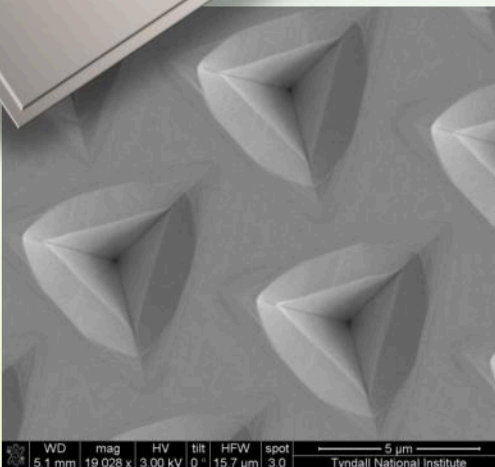
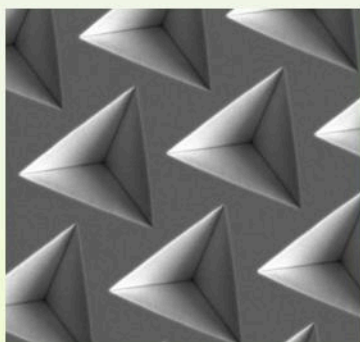


Post processing to enhance
extraction



“apex up” or
“back etching”,
prevents total
internal
reflection

**they are site-
controlled**



System of interconnected nanostructures*

AlGaAs growth

(In)GaAs growth

top view

side view

Ga-rich
AlGaAs
VQWR

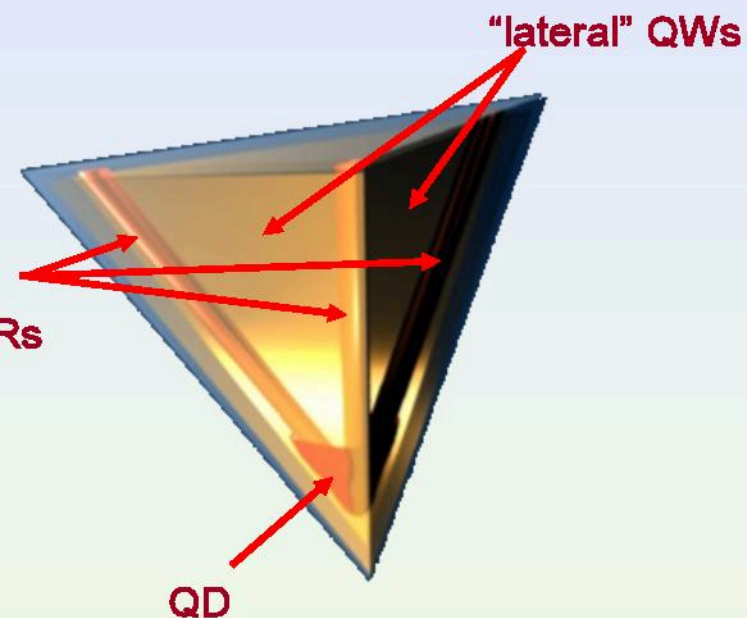
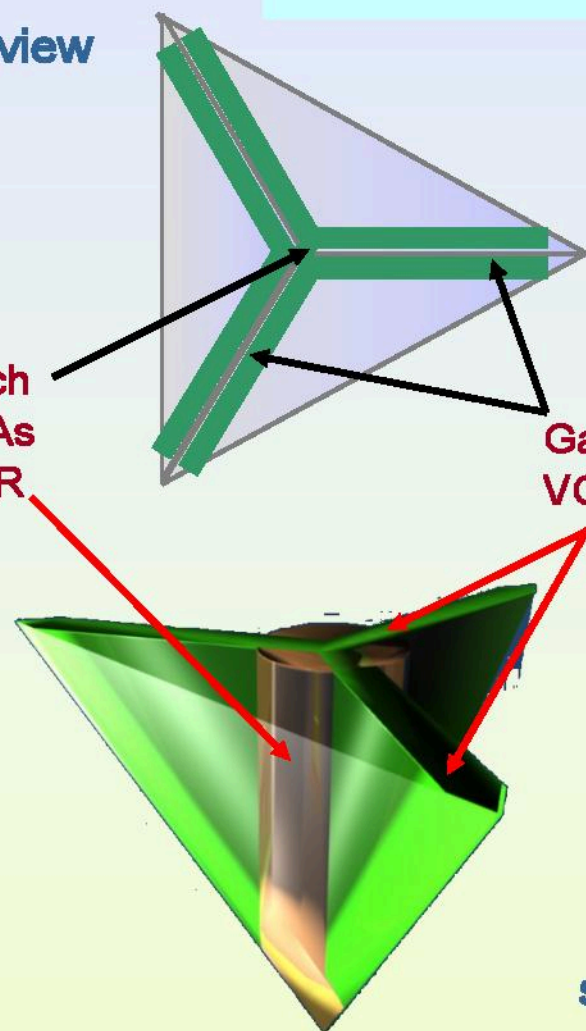
Ga-rich AlGaAs
VQW

"lateral" QWRs

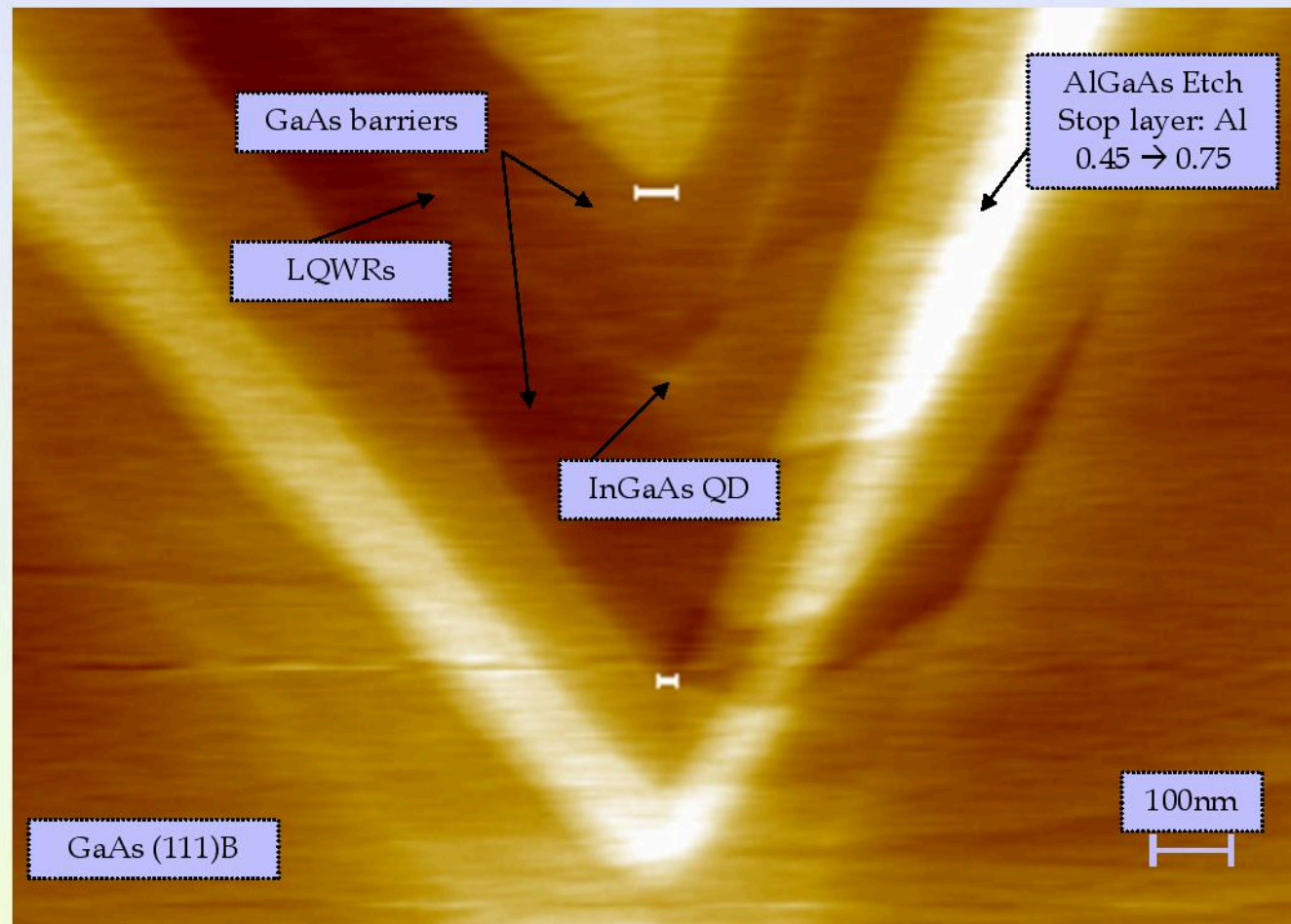
"lateral" QWs

QD

side view



InGaAs dots in GaAs barriers...



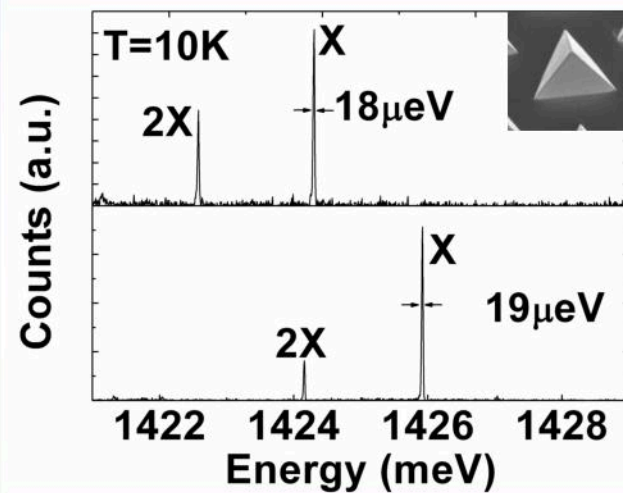
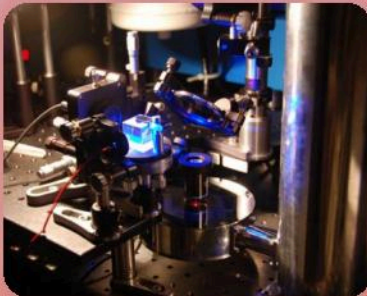
1.5 nm
 $\text{In}_{0.25}\text{Ga}_{0.75}\text{As}$ dot
in GaAs barriers

AFM cross section

Purity and uniformity (typically ~ 4 meV)...

Record linewidths for any site-controlled dots

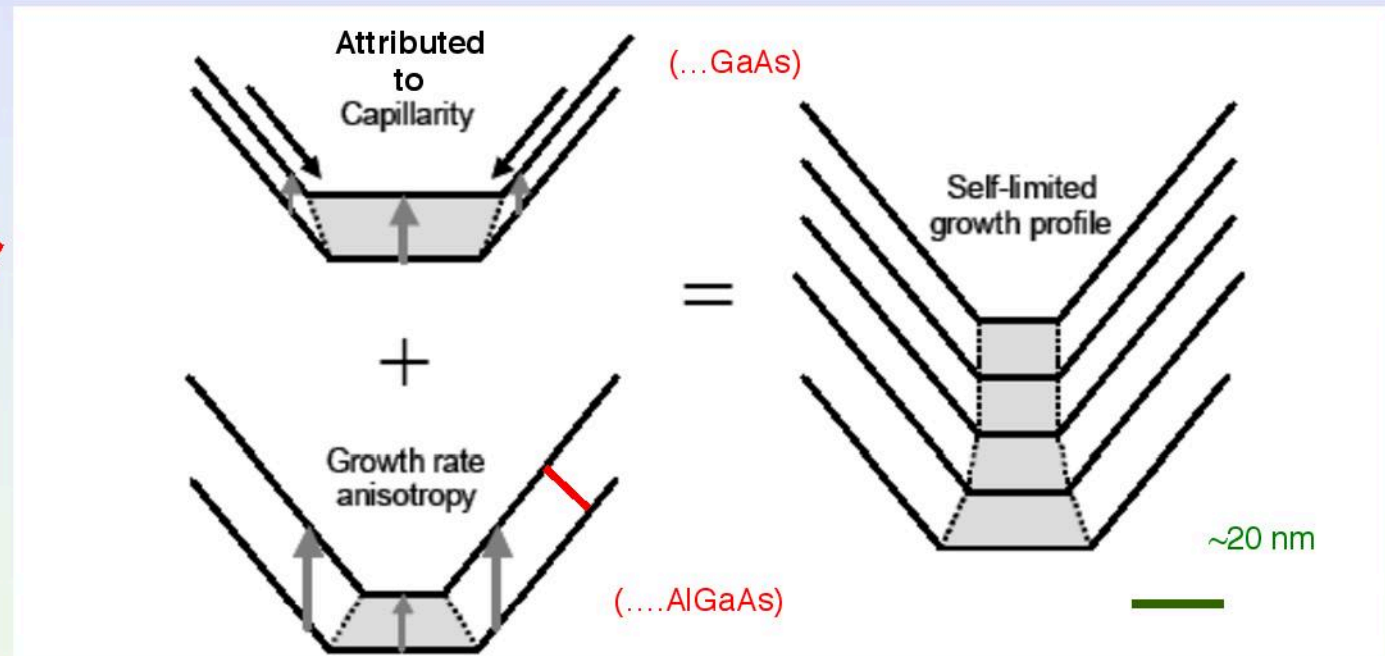
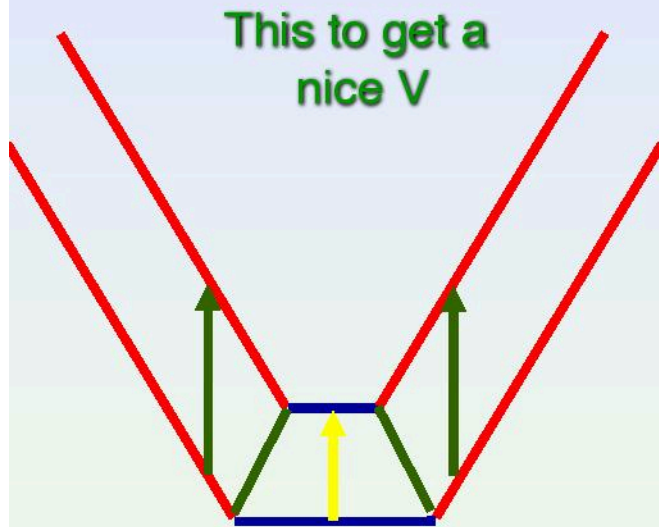
10 Kelvin!!!!



Best numbers to date, non resonant pumping, measured using interferometry: $\sim 10\mu\text{eV}$

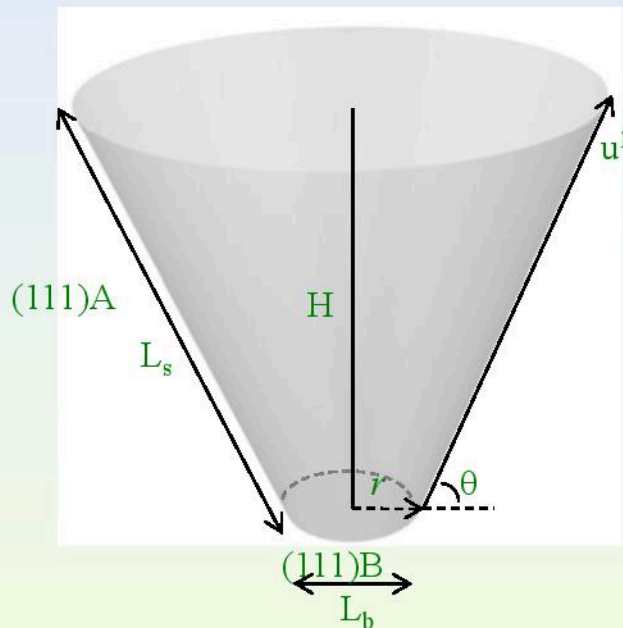
L.O. Mereni, V. Dimastrodonato, R.J. Young and E. Pelucchi, Appl. Phys. Lett. 94, 223121 (2009).

How they grow...like in V-grooves quantum wires....



Lateral growth rate much stronger than on bottom
Sidewalls grow faster...
So called capillarity..(but may be it is capillarity, may be not...)

In 3D... (similarly in 2D): it gives 2D diffusion , which one solves for stationary solution putting appropriate boundary conditions (111B/111A)



$$\nabla \cdot \mathbf{J}_i + F_i - \frac{n_i}{\tau_i} = 0 \quad \mathbf{J}_i = -D_i \nabla n_i$$

Decomposition rate anisotropy: $r = \frac{F_s}{F_b} > 1$

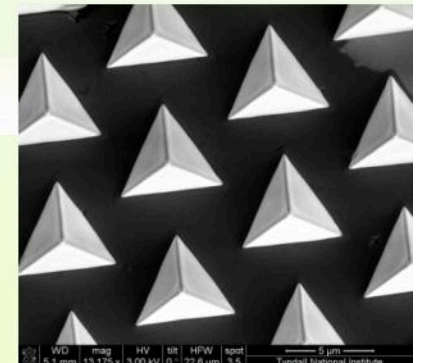
Surface diffusion (+ “capillarity”): $D_i = a^2 \nu \exp(-E_i^D/k_B T_G)$

Incorporation rate: $\tau_i = C_\tau \exp(E_i^\tau/k_B T_G)$

$$R_i = \frac{dz_i}{dt} = \Omega_0 \frac{n_i}{\tau_i}$$

Precursors decomposition only appear as an extra deposition flux, $F...$

V. Dimastrodonato, E. Pelucchi, and D. D. Vvedensky, “Self-limiting profile evolution of seeded two- and three- dimensional nanostructures during metalorganic vapour-phase epitaxy”, Phys. Rev. Lett. 96, 130501 (2012).



***Why it is not too bad to call QDs
artificial atoms....***

So, entangled photons....not our idea..since dots are “artificial atoms”...

One can use the transition from a “singlet state” (an “entangled” state because of indistinguishability, text book physics)

Just considering the two electrons

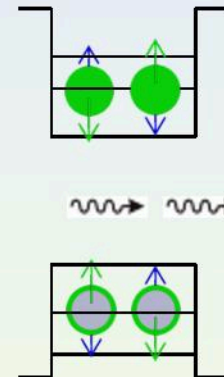
$$\frac{1}{\sqrt{2}}(|0\rangle|1\rangle - |1\rangle|0\rangle)$$

Two exchangeable electrons,
and two exchangeable holes...

appropriate parity under particle exchange



BiExcitonic State: 2X, two degenerate levels
antisymmetric state

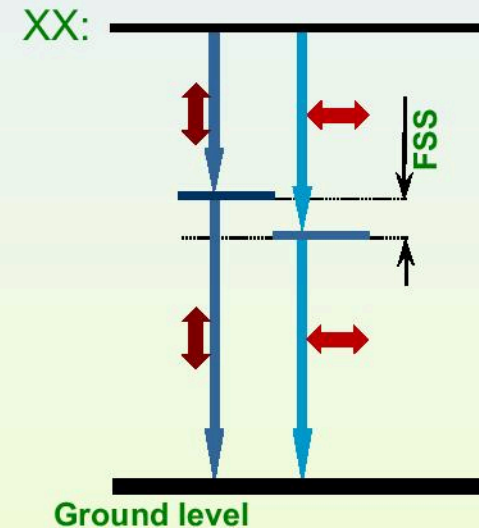
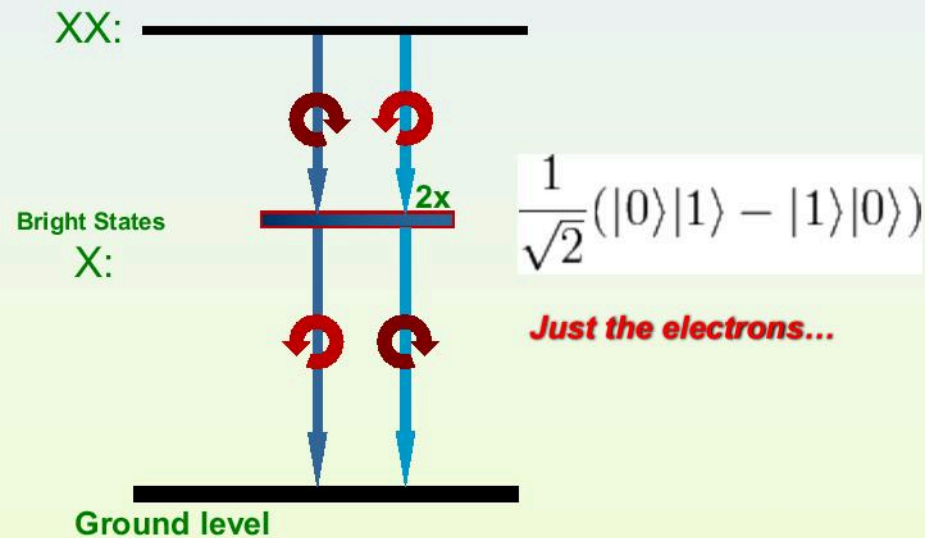


It has been done with real atoms in the early seventies..

$$|\psi\rangle = \frac{1}{\sqrt{2}}(|L_{XX}R_X\rangle + |R_{XX}L_X\rangle)$$

It is clear from what I said that a biexciton (and not only one confined in a dot) is **not a separable state**

(D. A. Kleinman Phys. Rev. B 28, 871 (1983) and many more)



Long story short if you have FSS...

$$|\psi\rangle = \frac{1}{\sqrt{2}} \left(|HH\rangle + e^{i2\pi FSS\tau / h} |VV\rangle \right)$$

R. Mark Stevenson et al. Phys Rev. Lett. 101, 170501 (2008)

When a FSS splitting is present the state tomography procedure averages over several randomly distributed/emitted different entangled states, practically resulting in an apparent classical state..... one is left with a statistical mixture...

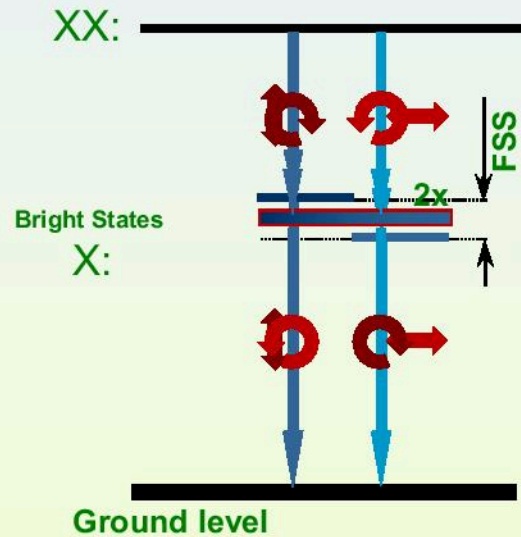
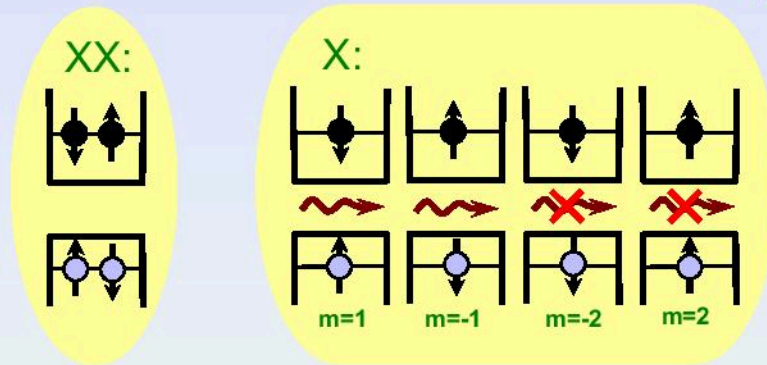
So, long story short: it is easier with a symmetric dot to “see” the entanglement

Pyramids should have C_{3V} symmetry which should ensure suppression of the FSS.

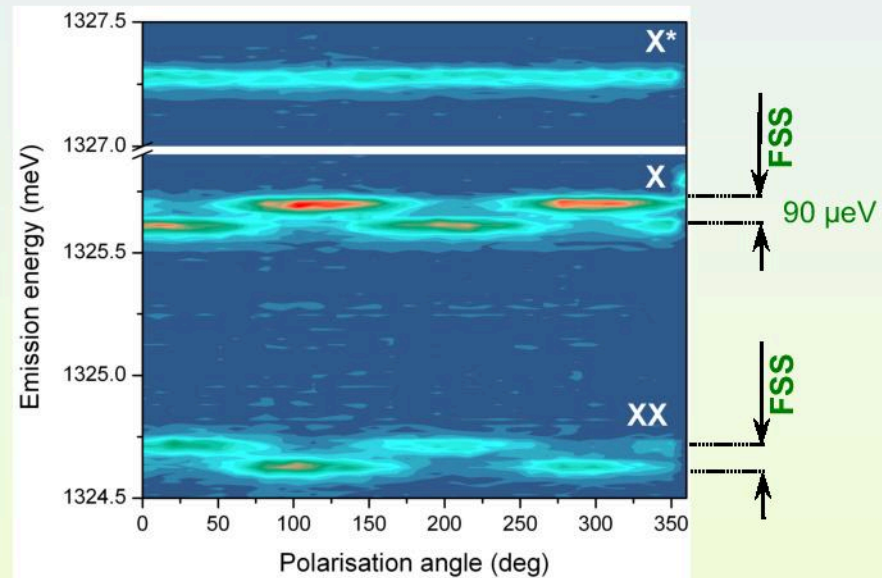
Singh, R., et al. Phys. Rev. Lett., 2009, 103(6),

Schliwa, A., et al. Phys. Rev. B, 2009, 80(16),

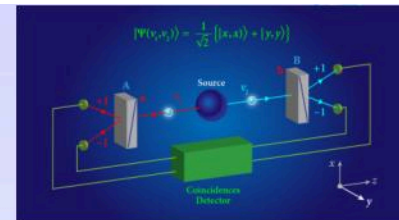
Karlsson, K.F., et al. Phys. Rev. B, 2010, 81(16).



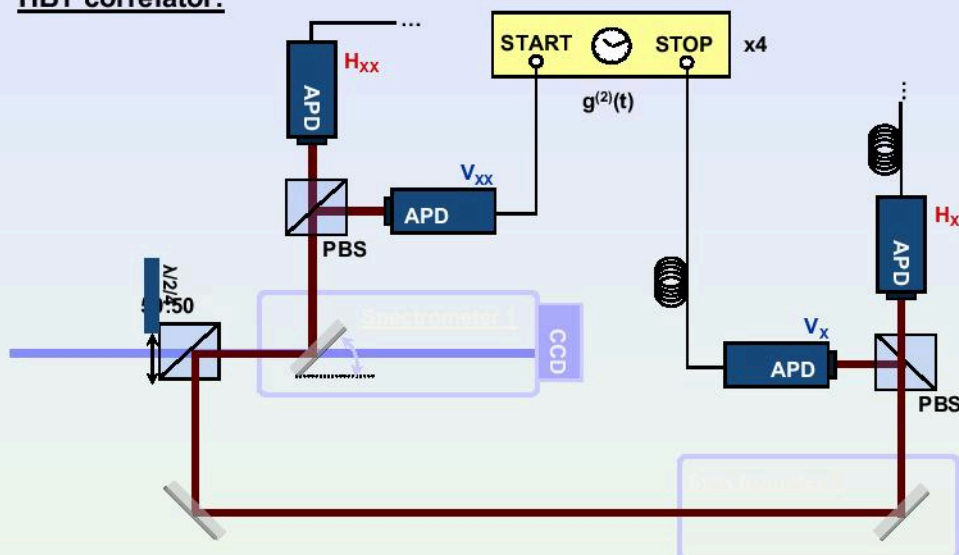
Low temperature grown, 1.2 nm InGaAsN QD:



Polarization-entangled photon emission



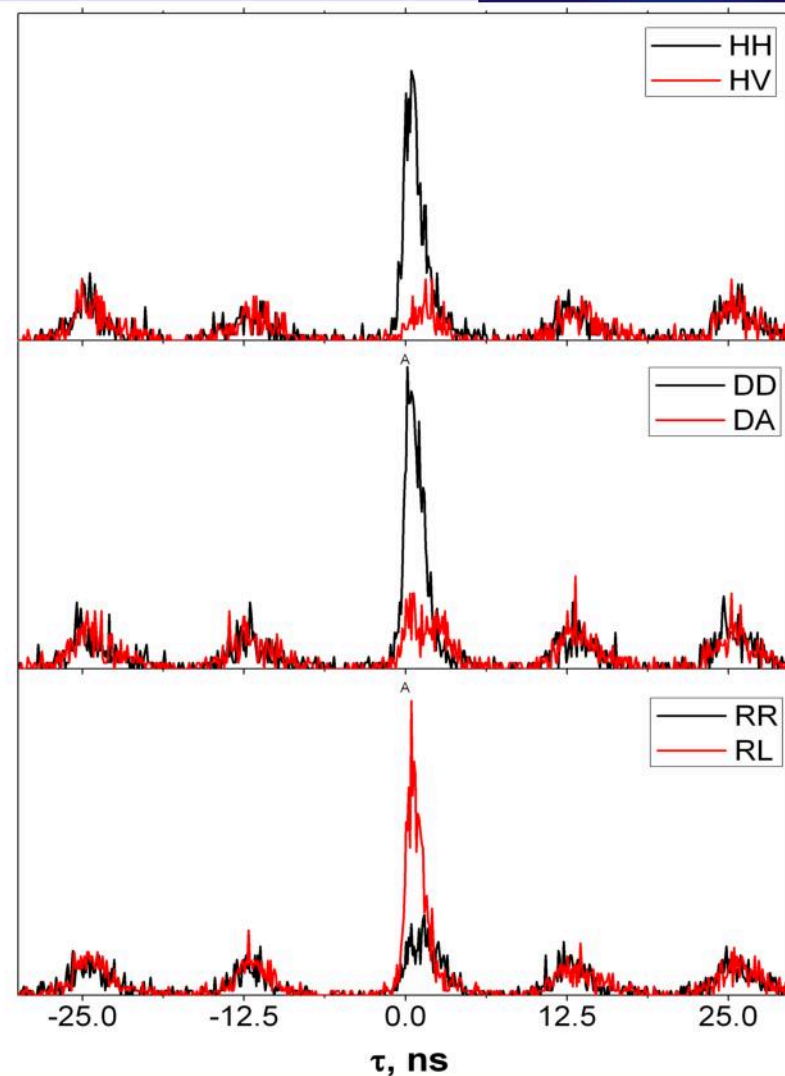
HBT correlator:



$$\begin{aligned} |A\rangle &= \frac{1}{\sqrt{2}}(|H\rangle - |V\rangle) \\ |D\rangle &= \frac{1}{\sqrt{2}}(|H\rangle + |V\rangle) \\ |L\rangle &= \frac{1}{\sqrt{2}}(|H\rangle - i|V\rangle) \\ |R\rangle &= \frac{1}{\sqrt{2}}(|H\rangle + i|V\rangle) \end{aligned}$$

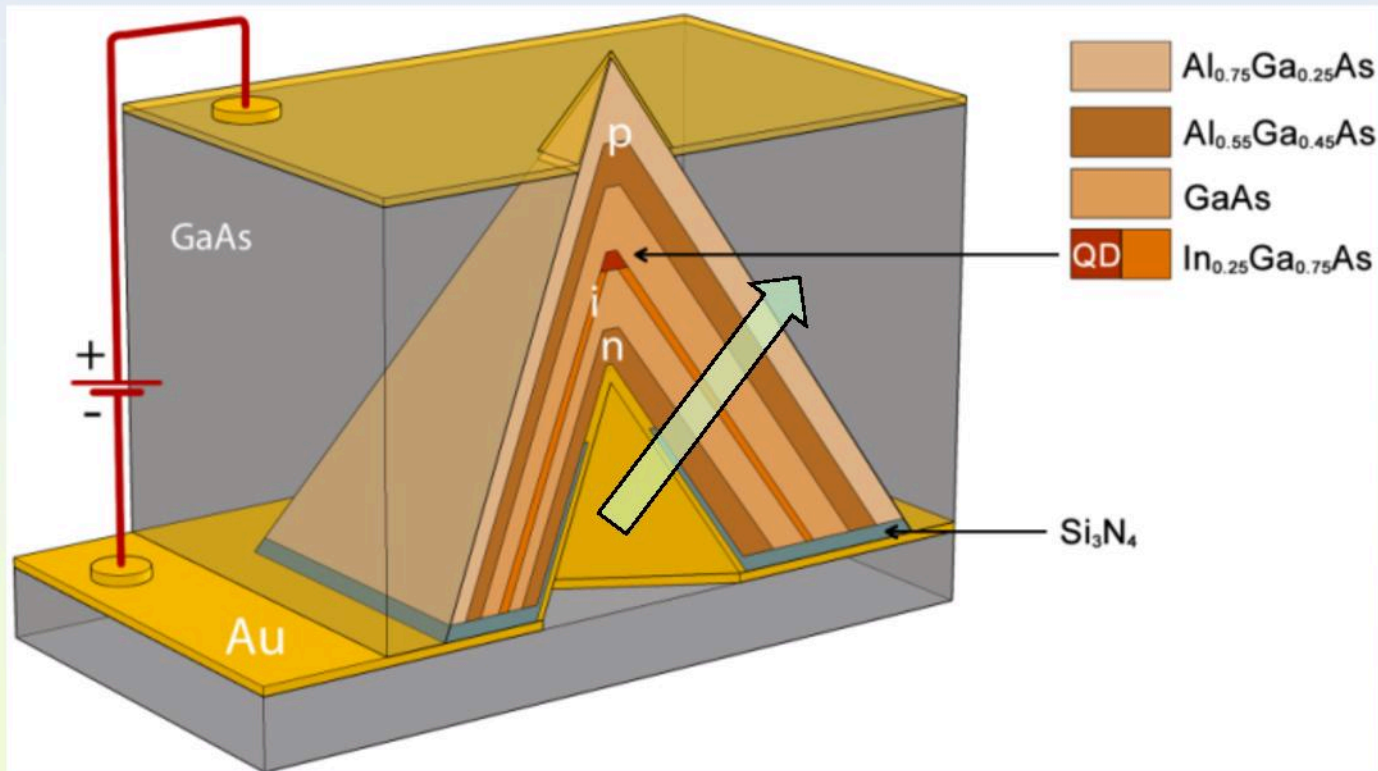
$$\begin{aligned} |\psi\rangle &= \frac{1}{\sqrt{2}}(|L_{XX}R_X\rangle + |R_{XX}L_X\rangle) = \\ &= \frac{1}{\sqrt{2}}(|H_{XX}H_X\rangle + |V_{XX}V_X\rangle) = \\ &= \frac{1}{\sqrt{2}}(|D_{XX}D_X\rangle + |A_{XX}A_X\rangle) \end{aligned}$$

$g^{(2)}(\tau)$



Can we electrically inject?

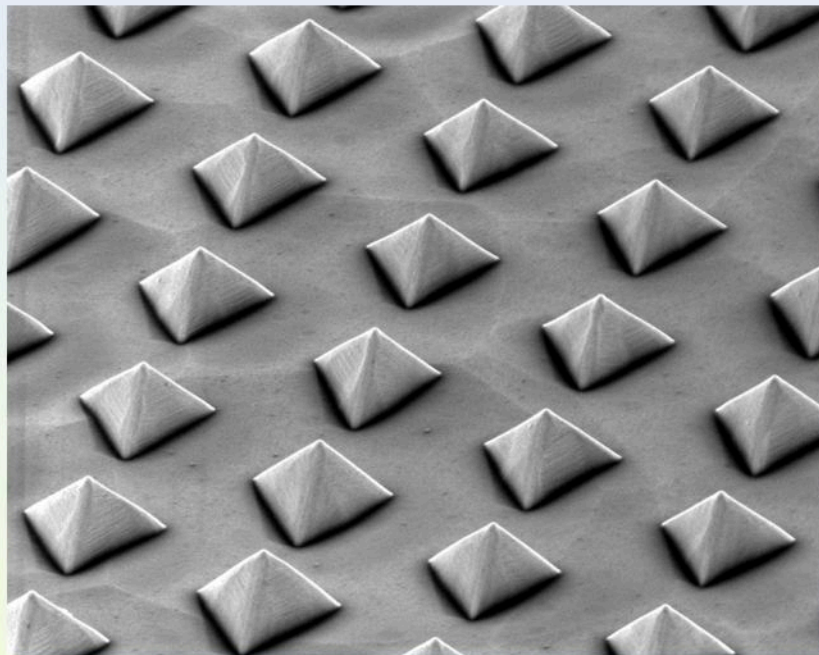
If you think about it, it should not work.....



Current prefers to go through the sides...shorter path (a factor of 3 or so!!!)..

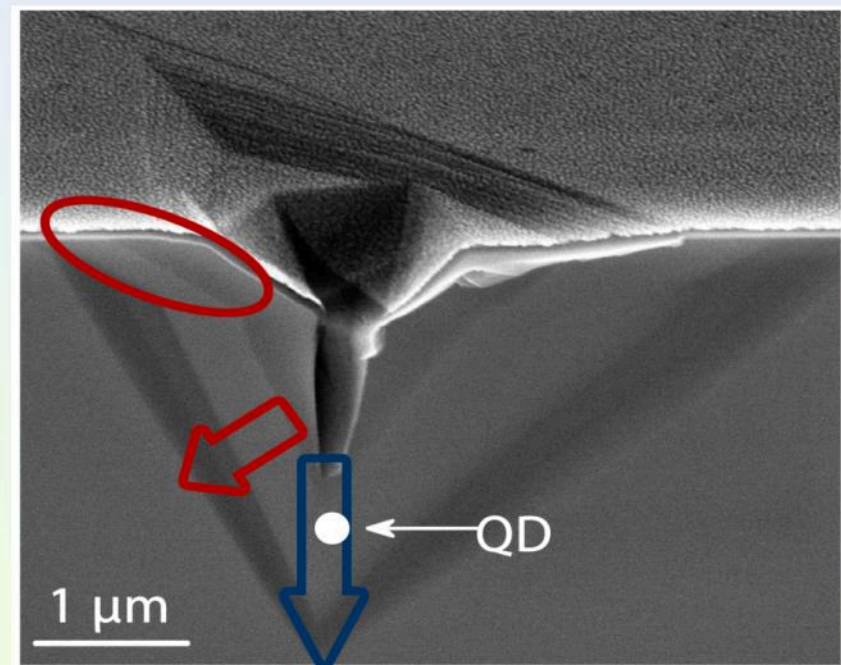
Device fabrication....issues

Apex-up geometry is essential to ensure high light extraction efficiency.

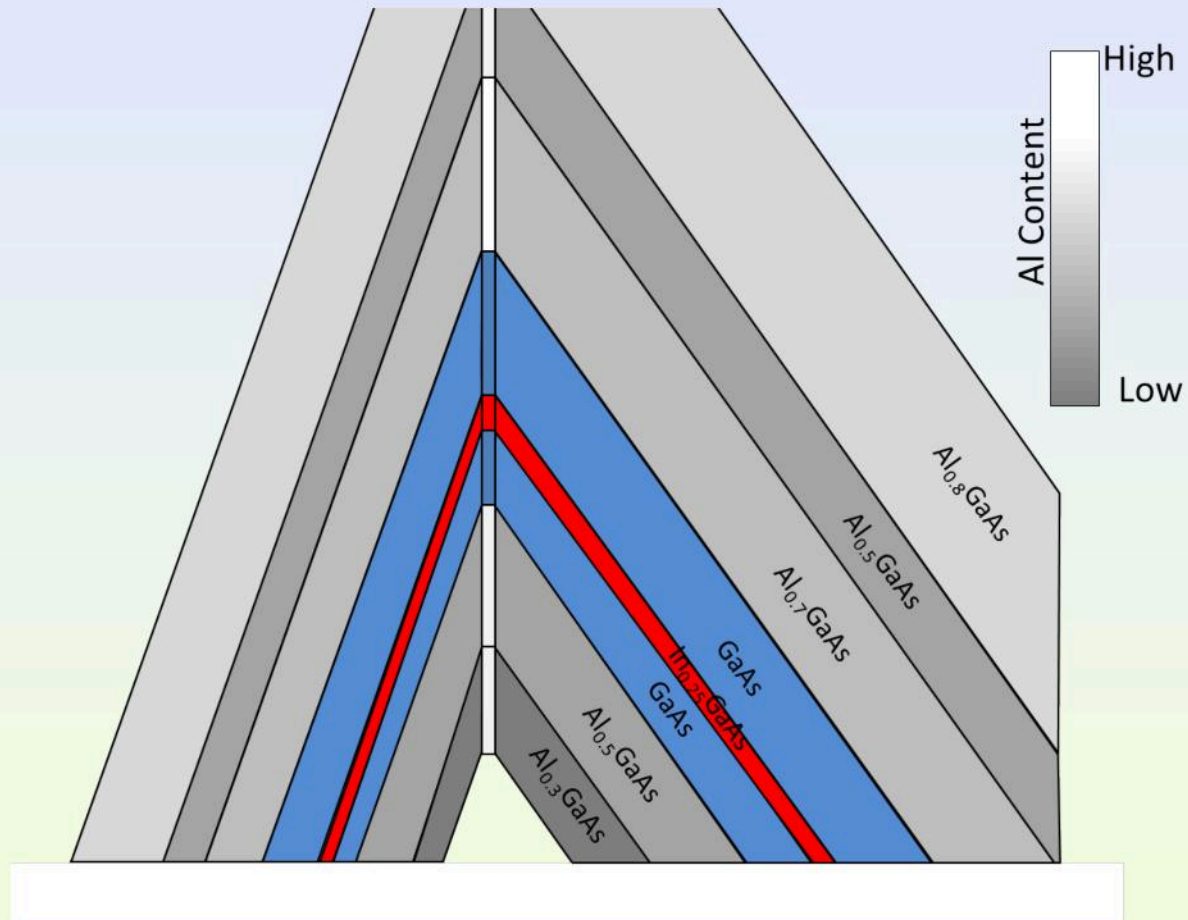
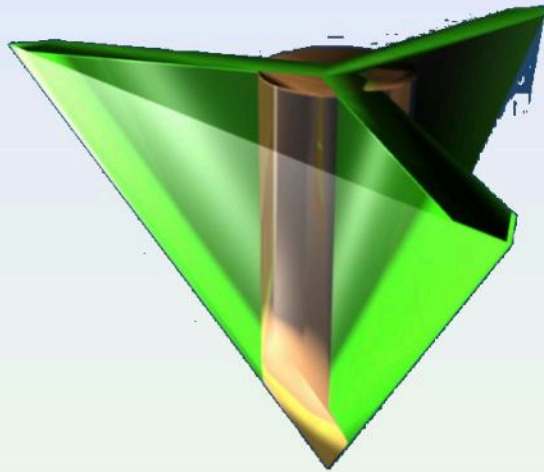


Issues:

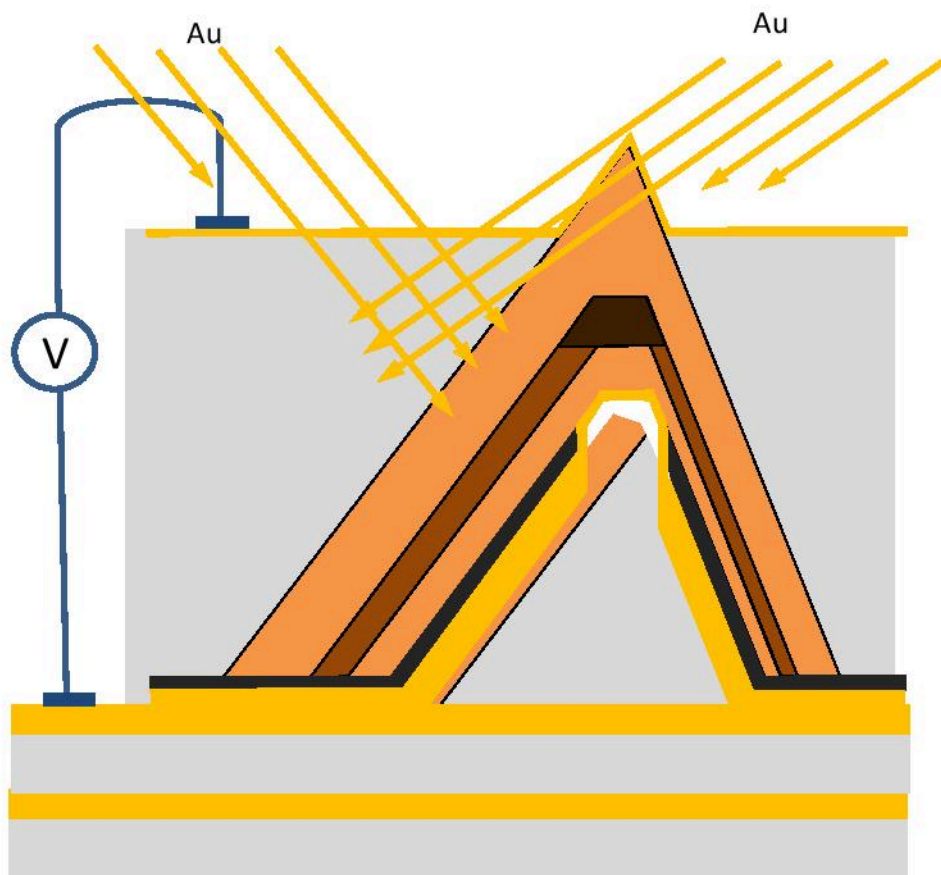
- Non-planar structure
- Current leakage outside QD region



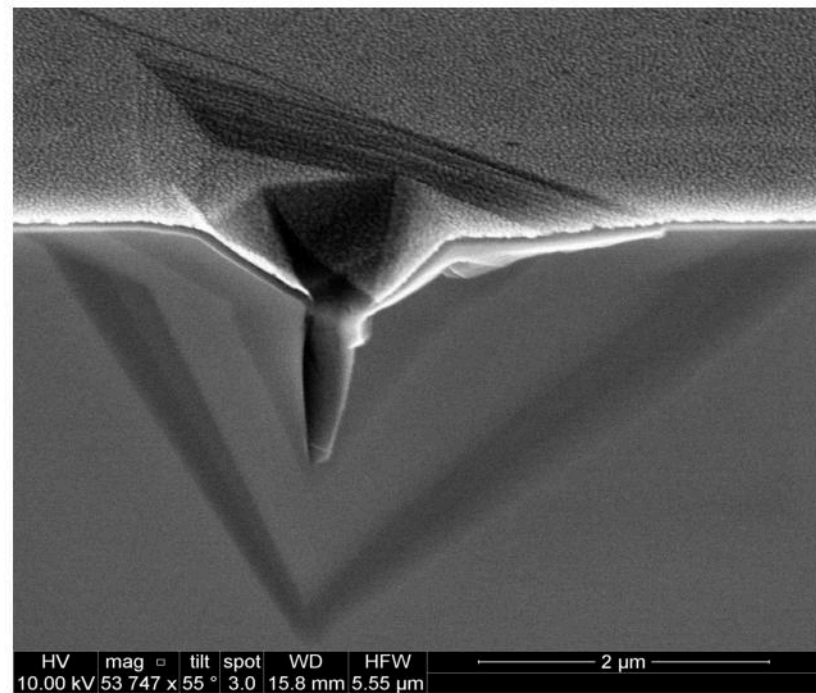
How to make it work... engineered injection... VQWR..



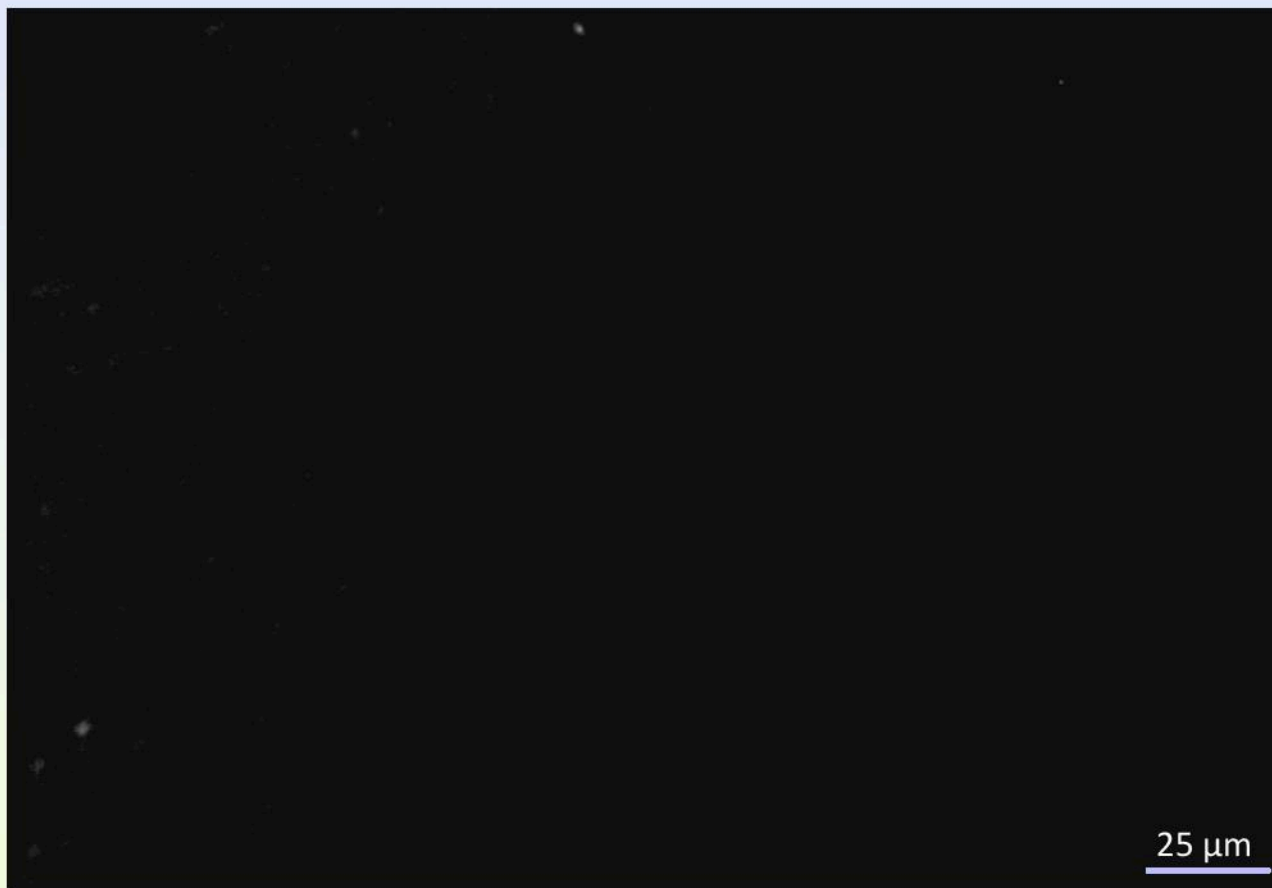
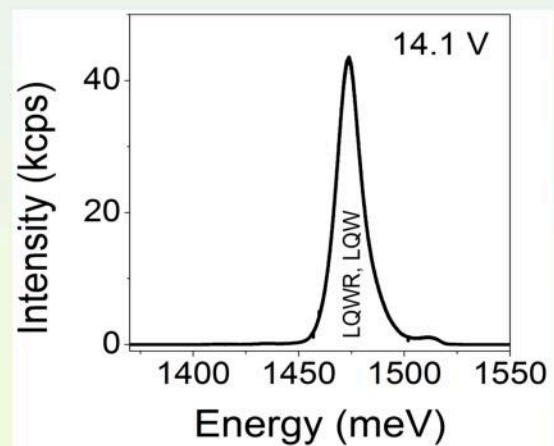
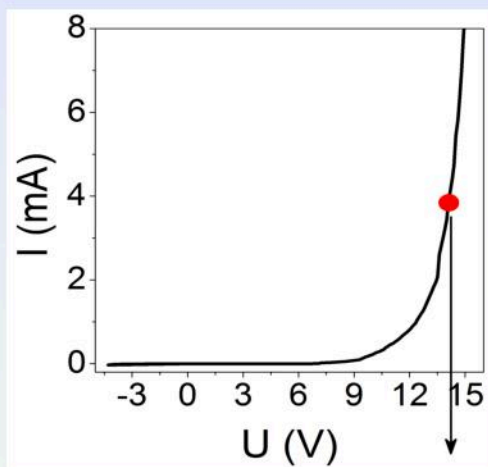
Diode processing



LED production steps:

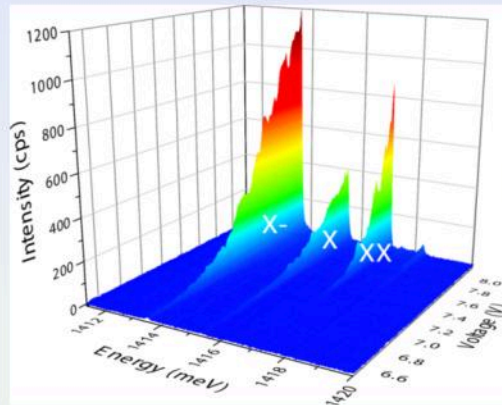


Electroluminescence

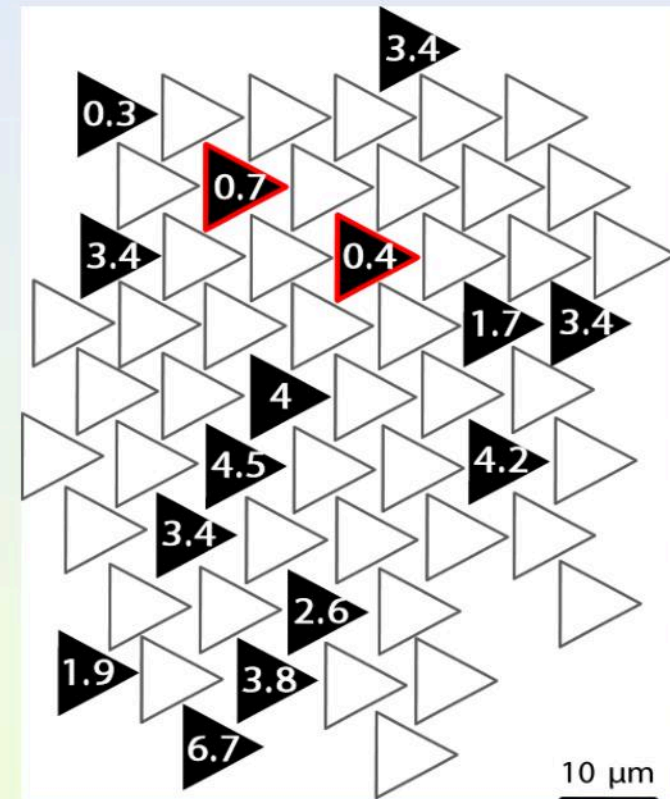


Symmetry

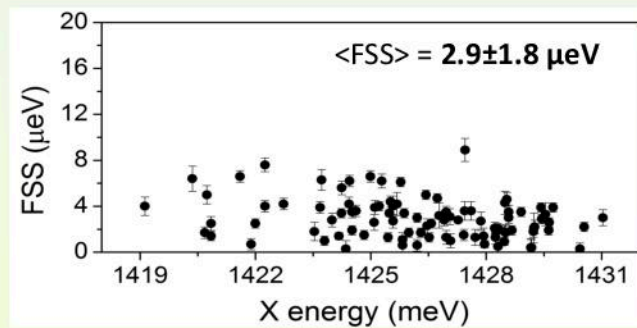
- A single QD electro-luminescence



- Functional μ LED distribution and FSS values

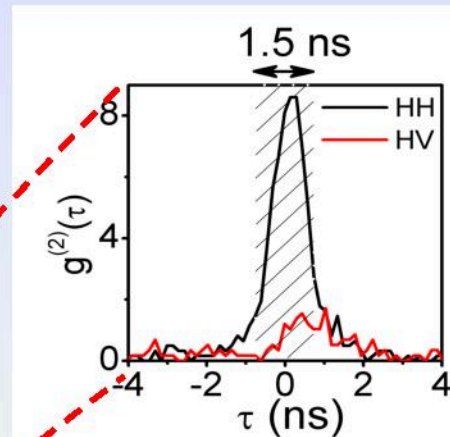
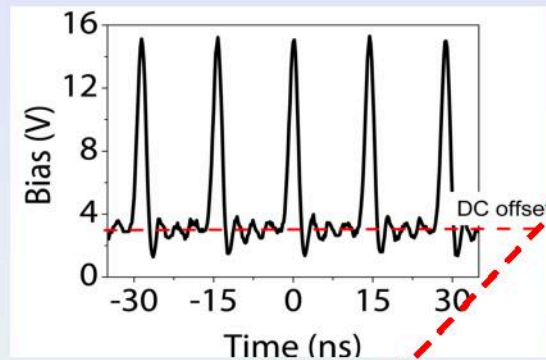


- FSS values



Triggered entangled photon emission

- Pulsed injection:



- Simplified estimations of Bell's inequality:
(Young, R. J. PRL **102**, 030406, 2009)

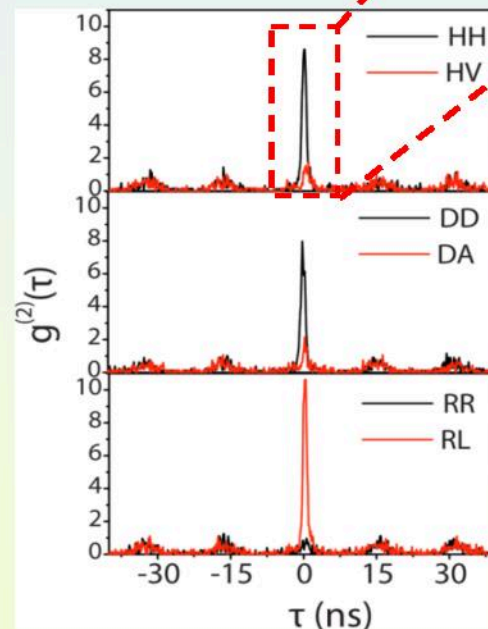
$$S_{RC} = \sqrt{2}(C_R - C_C) \leq 2$$

$$S_{RD} = \sqrt{2}(C_R + C_D) \leq 2$$

$$S_{DC} = \sqrt{2}(C_D - C_C) \leq 2$$

$$C_{basis} = (g_{xx,x}^{(2)} - g_{xx,\bar{x}}^{(2)}) / (g_{xx,x}^{(2)} + g_{xx,\bar{x}}^{(2)})$$

- Correlations:

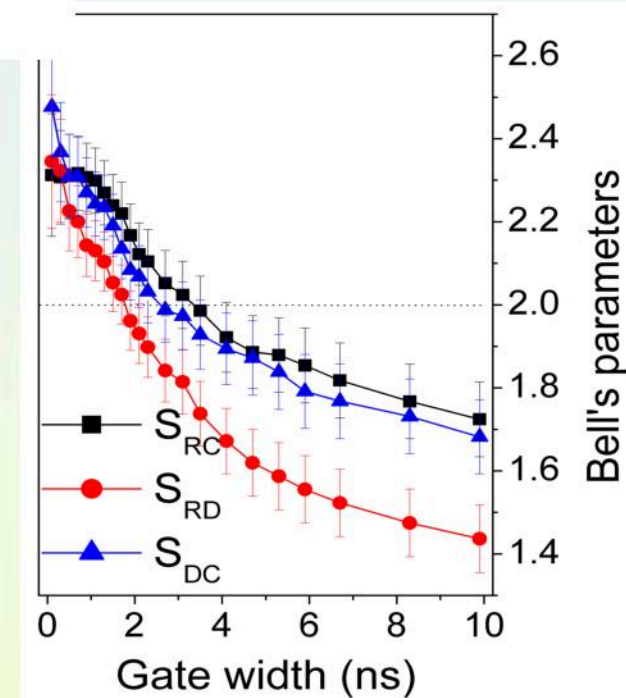


With 1.5 ns window and
75% intensity preserved:

$$S_{RD} = 2.053 \pm 0.070$$

$$S_{DC} = 2.191 \pm 0.075$$

$$S_{RC} = 2.239 \pm 0.074$$



nature
photonics

Selective pyramidal light-emitting

T. H. Chung[†], G. Jus

Scalability and foundry c
in developing quantum t
technology that has the
arrays of electrically dri
The design of the sou
crystallographic directio
bright entangled-photon
density of light-emitting
inequality. Compatibility
make these devices attra

nature photonics

DECEMBER 2016 VOL 10 NO 12
www.nature.com/naturephotonics

Scalable sources
of entanglement

OPTOMECHANICS
Single-photon frequency shifter

MODULATORS
Switchable anti-laser

MICROSCOPY
Super-resolution holography

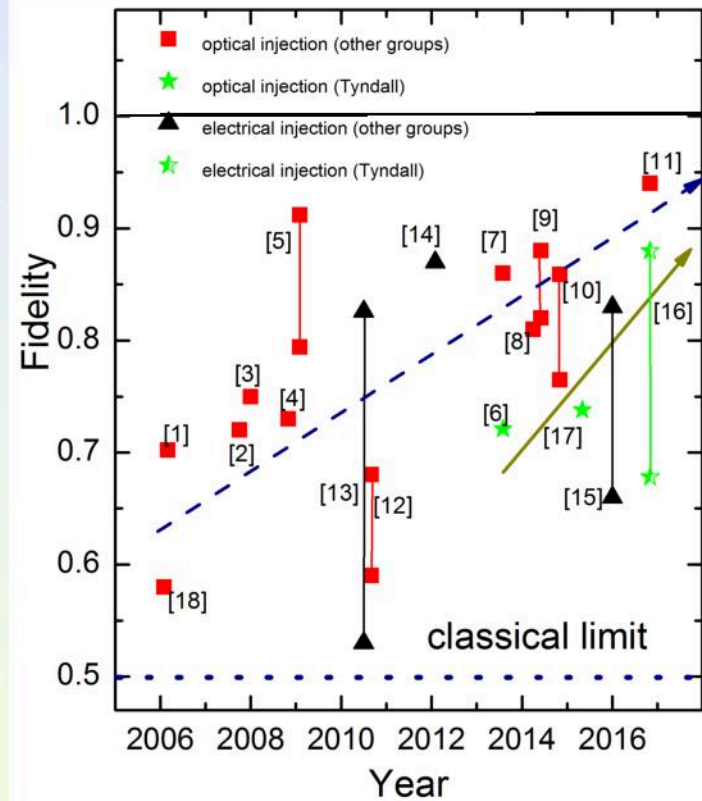
ARTICLES

038/NPHOTON.2016.203

arrays of photon

processors, for example)
duce a quantum photonic
site-controlled, scalable
e quantum information.
al recesses along the
ots—a requirement for
structures allows a high
that also violate Bell's
graphic position control
processing.

Where are we going with QDs?

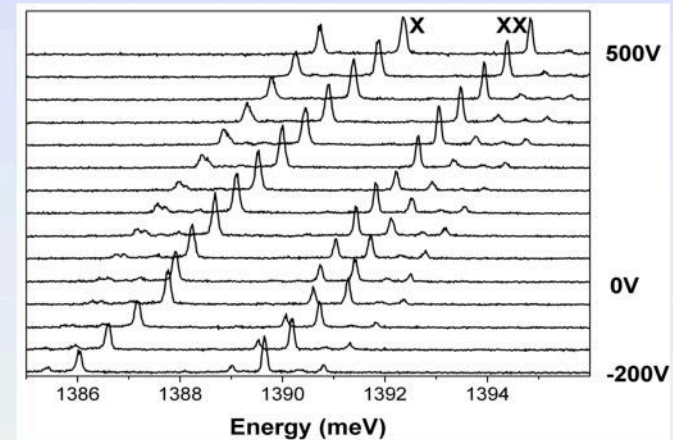


Short term future

Integration of QDs on piezoelectric actuators:

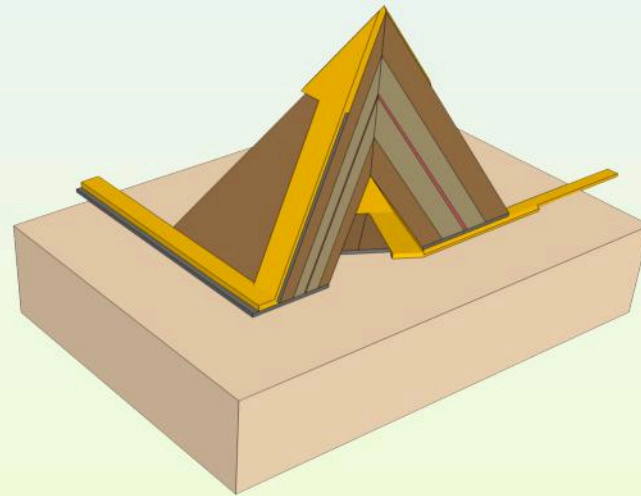
- Tuning emission energy.
- Tuning the fine-structure splitting.

Collaboration with JKU Linz (A. Rastelli, R. Trotta, et al.)

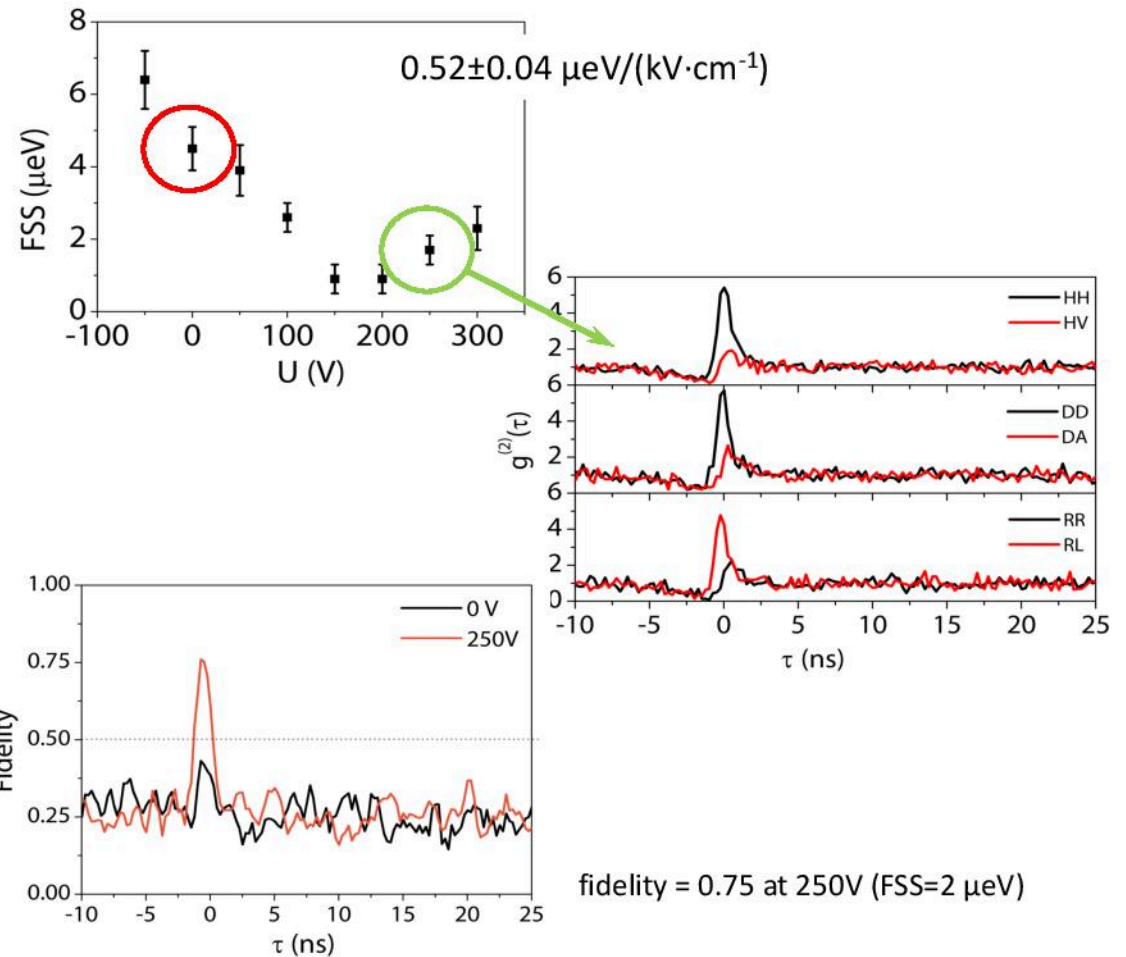
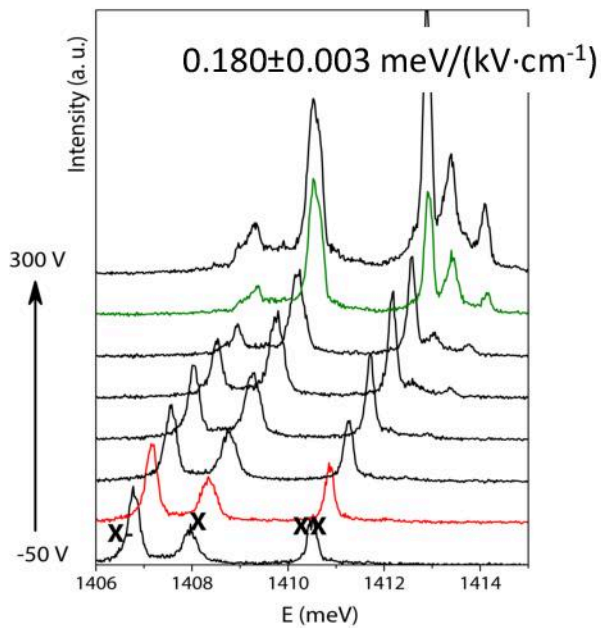
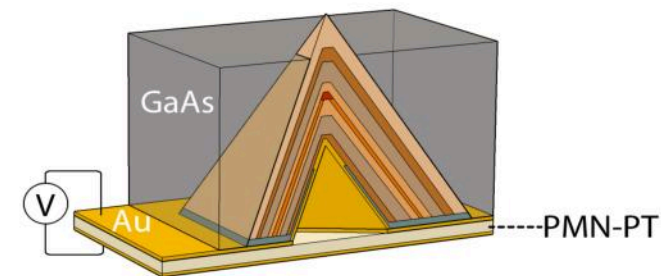


Adding local metallic contacts:

- Electric injection of carriers.
- Tuning emission energy.
- Tuning the fine-structure splitting.
- Electrical manipulation of spins.



Energy and FSS tuning: biaxial strain



EP Epitaxy and Physics
of Nanostructures

IPIC
BRINGING PHOTONICS TO LIFE

sfi
science foundation ireland
fondúireacht eolaíochta éireann

